A formal methodology for avoiding hyperstaticity when connecting an exoskeleton to a human member

Nathanaël Jarrassé
Guillaume Morel

Université P. et M. Curie Paris VI, ISIR (Institut des Systèmes Intelligents et de Robotique) CNRS - UMR 7222
4 place Jussieu, 75005 Paris - France
Telephone: +33.1.44.27.51.41
Emails : jarrasse@isir.fr, guillaume.morel@upmc.fr

***Abstract*— The design of a robotic exoskeleton often focuses on replicating the kinematics of the human limb that it is connected to. However, human joint kinematics is so complex that in practice, the kinematics of artificial exoskeletons fails to reproduce it exactly. This discrepancy results in hyperstaticity. Namely, uncontrolled interaction forces appear.**
In this paper, we investigate the problem of connecting an exoskeleton to a human member while avoiding hyperstaticity; to do so, we propose to add passive mechanisms at each connection point.
First, analyzing the twist spaces generated by these fixation passive mechanisms, we provide necessary and sufficient conditions for a given *global isostaticity condition* to be respected. Then, we derive conditions on the number of Degrees of Freedom (DoFs) to be freed at the different fixations, under full kinematic rank assumption.
We finally apply the general methodology to the particular case of a 4 DoF shoulder-elbow exoskeleton. Experimental results allow to show an improvement in transparency brought by the passive mechanism fixations.

I. Introduction

Whatever the particular use they are designed for (augmenting human force capabilities, helping a patient during a neurophysical rehabilitation, haptic or master device, etc.), the major purpose of exoskeletons is to transmit forces to the connected human limb. Designing these physically connected devices faces a rather challenging set of constraints: adaptability to kinematics variations between human subjects is required; large force capability is desirable over a large workspace; simultaneously transparency (i.e. capability of applying minimal forces in resistance to the subject's movements) is of high importance. Designing the kinematics of an exoskeleton consists of trying to replicate the human limb kinematics. This brings a number of advantages: similarity of the workspaces, singularity avoidance [1], natural feeling of the connection with human subject. If the kinematics of the human limb and the exoskeleton are the same, there is a one-to-one mapping between the joint torques exerted by the robot and the joint torques applied to the human subject, whatever the joint configuration.

A major drawback of the exoskeleton paradigm is that, in fact, human kinematics is impossible to replicate with a robot. Two problems occur: morphology drastically varies by the subject and, for a given subject, the joints kinematics is very complex and cannot be imitated by conventional robot joints [2]. In fact, it is impossible to find any consensual model of the human kinematics in the biomechanics literature due to complex geometry of bones interacting surfaces. For example, different models are used for the shoulder-scapula-clavicle group[3].
Since human limb models are only approximations, exoskeletons are imperfect. This generates kinematic compatibility problems. Indeed, when connecting two-by-two the links of two *kinematically similar* chains that are not perfectly identical, hyperstaticity occurs. This phenomenon leads, if rigid models are used, to the impossibility of moving and the appearance of non-controllable (possibly infinite) internal forces. In practice, though, rigidity is not infinite and mobility can be obtained thanks to deformations. When a robotic exoskeleton and a human limb are connected, most likely, these deformations occur at the interface between the two kinematic chains, caused by the low stiffness of skin, tissues. Solutions found in the literature to cope with problem are of two kinds.
Firstly the exoskeleton design can be thought in such a way that adaptation to human limb kinematic is maximized: robotic segments with adjustable length were developed, pneumatic systems were added to introduce elasticity in the robot fixations and adaptability to variant limb section [4]. All these approaches add to the exoskeleton complexity while they are not formally proven to solve the hyperstaticity problem. No quantification is shown.
Secondly, keeping the exoskeleton structure unchanged, one can add passive DoF at the connections between the robot and the limb. Indeed, in closed chain mechanisms, adding joints is a way of deceasing the degree of hyperstaticity. Several attempts can be found in the literature ([**?**], [**?**]) but remain mostly empirical with no formal statement on the degree of

hyperstaticity.
Rather, thanks to basic theory of mechanisms, we consider in this paper the general problem of limb-exoskeleton connections and derive a formally proved set of conditions (Section I). In Section II, the method is applied to ABLE, a 4 active DoF arm exoskeleton. In Section III, the experimental setup for the fixation evaluation is described and finally in Section IV, results of preliminary evaluation of these isostatic fixations are presented and discussed.

II. General Methodology

The main question addressed in this paper is: given a proposed orthotic structure designed to (approximately) replicate a human limb kinematic model, how to connect it to the human limb while avoiding the appearance of uncontrollable forces at the interface? The answer takes the form of a set of passive frictionless mechanisms used to connect the robot and the subject's limb that allows to avoid hyperstaticity.

A. Problem formulation

We consider two different serial chains with multiple couplings as illustrated in Fig. 1. One represents an human limb **H** and the other the robot structure **R**.

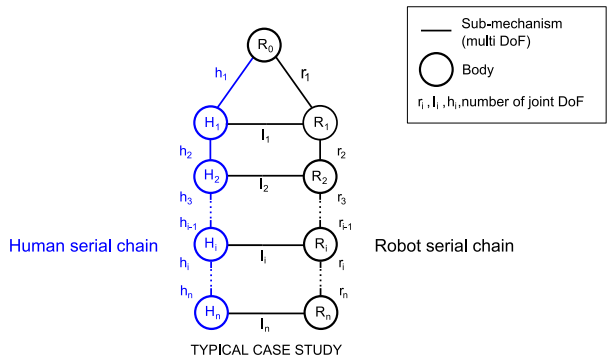

Fig. 1. Schematic of two serial chains parallel coupling

The base body of the exoskeleton is supposed to be attached to a body of the human subject. This common body is denoted $\mathscr{R}_0 \equiv \mathscr{H}_0$. The robot and the limbs are supposed to be connected through n fixations. Each fixation mechanism $\mathbf{L}_i$ for $i \in \{1,..,n\}$ is a passive kinematic chain which connects a human body $\mathscr{H}_i$ to a robot body $\mathscr{R}_i$. Mechanisms $\mathbf{L}_i$ are supposed to have possess a connectivity l_i. Recall that connectivity is the minimum and necessary number of joint scalar variables that determine the pose of the $\mathbf{L}_i$ chain [5]. Typically, $\mathbf{L}_i$ can be a nonsingular serial combination of l_i one DOF joints. The fixation can be an embedment ($l_i = 0$) or can liberate several DOF, such that:

$$\forall i \in \{1,..,n\}, \quad 0 \leq l_i \leq 5 \quad . \tag{1}$$

Indeed choosing $l_i \geq 6$ would correspond to complete freedom between $\mathscr{H}_i$ and $\mathscr{R}_i$ which would not make any practical sense in the considered application where force transmission is required.

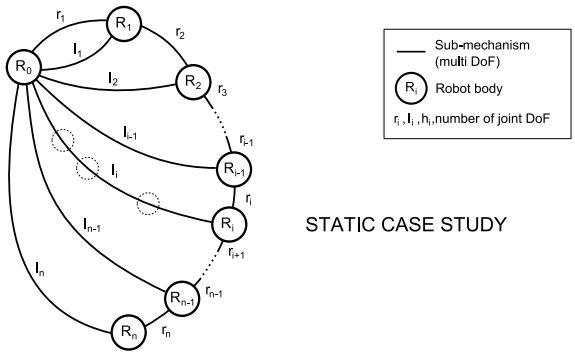

Fig. 2. Studied problem with a fixed human limb

Between $\mathscr{R}_{i-1}$ and $\mathscr{R}_i$, on the robot side, there is an active mechanism $\mathbf{R}_i$ which connectivity is denoted r_i. Similarly, between $\mathscr{H}_{i-1}$ and $\mathscr{H}_i$ on the human side, there is a mechanism $\mathbf{H}_i$ of connectivity h_i. Note that, due to the complexity of human kinematics h_i is not always exactly known, and literature from biomechanics provide controversial data on this point. For example, the elbow is often modeled as a one DOF joint, but in reality a residual second DOF can be observed [6].
Our goal is to design mechanisms $\mathbf{L}_i$ with $i \in \{1,..,n\}$ in such a way that on one side, all the forces generated by the exoskeleton on the human limb are controllable and on the other side, there is no possible motion for the exoskeleton when the human limb is still. We shall thus consider in the next that the human limbs are virtually attached to the base body $\mathscr{R}_0$. This represents the worst case for mobility, when the subject does not move at all. The resulting overall mechanism, depicted in Fig. 2, is denoted S_n.
A proper design for the passive mechanisms $\mathbf{L}_i$ shall guaranty that, in the absence of any external forces, both:

$$\forall i \in 1 \cdots n, \quad {}^{S_n}T_i = \{0\} \quad \textit{and} \tag{2a}$$

$$\forall i \in 1 \cdots n, \quad {}^{S_n}W_{li \to 0} = \{0\} \quad , \tag{2b}$$

where ${}^{S_n}T_i$ is the space of twists describing the velocities of robot body $\mathscr{R}_i$ relative to $\mathscr{R}_0$ in S_n and ${}^{S_n}W_{li \to 0}$ is the space of wrench statically admissible transmitted through the l_i chain on the reference body $\mathscr{R}_0$ (the blocked arm), i.e. the space of the forces (forces and moments) resulting from a possible hyperstatism appearing when S_n reaches the equilibrium.
Equation (2a) expresses the fact that the mobility of any robot body connected to a human limb should be null, which is required since the human member is supposed here to be still. Moreover, Eq. (2b) imposes that, considering the whole mechanism, there can be no forces of any kind exerted on the human limb. Indeed, since the actuators are supposed to apply a null generalized force, the presence of any force at the connection ports would be an uncontrollable force due to hyperstaticity.
Therefore, Eq. (2) is referred in the next as *global isostaticity condition*.

B. Conditions on the twist space ranks

We can notice the recursive structure of the considered system: if we name S_i the sub-mechanism constituted by the bodies $\mathscr{R}_0$ to $\mathscr{R}_i$ and the chains r_0 to r_i and l_0 to l_i, we can represent S_i recursively from S_{i-1}, see Fig. 3. In this

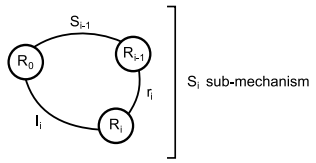

Fig. 3. Recursive structure S_i of the system

convention, S_0 represents a zero DoF mechanism. Using this recursive representation of the studied mechanism S_n easily leads to establish the following proposition:

Proposition 1: The conditions (2) are equivalent to :

$$\forall i \in 1 \cdots n, \quad dim(T_{S_{i-1}} + T_{r_i} + T_{l_i}) = 6 \qquad and \tag{3a}$$

$$\forall i \in 1 \cdots n, \quad dim(T_{r_i} \cap T_{l_i}) = 0 \qquad and \tag{3b}$$

$$dim(T_{S_n}) = 0 \quad , \tag{3c}$$

where $T_{S_j} = {}^{S_j}T_j$ is the space of twists describing the velocities of robot body $\mathscr{R}_j$ relative to $\mathscr{R}_0$ in S_j (then it is different from ${}^{S_n}T_j$), T_{r_i} is the space of twists produced by $\mathbf{R}_i$ – *i.e.* the space of twists of $\mathscr{R}_i$ relative to $\mathscr{R}_{i-1}$ if they were only connected trough $\mathbf{R}_i$, T_{l_i} is the space of twists produced by the l_i chain *i.e.* the space of twists of $\mathscr{R}_i$ relative to $\mathscr{R}_0$ if they were only connected through $\mathbf{L}_i$. ■

The demonstration can be found in the appendix.

In order to make these necessary and sufficient conditions of any help for the design of $\mathbf{L}_i$, it is required to derive a set of conditions on the connectivities l_i (the number of DOF). This is done in the next.

C. Conditions on connectivities

Firstly, one has:

$$(3a) \Rightarrow \forall i \in 1 \cdots n, \quad m_{i-1} + r_i + l_i \geq 6 \tag{4}$$

with $m_i = dim(T_{S_i})$. This condition comes directly from the fact that, from any vector subspaces **A**,**B** and **C** of a vector space **E**, $dim(\mathbf{A}+\mathbf{B}+\mathbf{C}) \leq dim(\mathbf{A}) + dim(\mathbf{B}) + dim(\mathbf{C})$.

Secondly:

$$(3b) \Rightarrow \forall i \in 1 \cdots n, \quad m_{i-1} + r_i \leq 6 \tag{5}$$

This condition come from the fact that if **A** and **B** are two vector subspaces of **E** and $dim(\mathbf{A}) + dim(\mathbf{B}) > dim(\mathbf{E})$, then$\mathbf{A} \cap \mathbf{B} \neq \{0\}$.

Finally:

$$(3c) \Rightarrow m_n = 0 \tag{6}$$

At this stage, it is important to notice that Eq. (4,5,6) express only necessary conditions on l_i, m_i and r_i. These conditions are not sufficient since any particular configuration of the axes that would decrease the rank of any kinematic equation for S_n would change the dimension of the combined space of twists. We will assume, in the next, that such singularities are avoided, which is of course to be verified a posteriori when considering a particular design.

This assumption allows to derive a relationship m_i and l_i and r_i. One has:

$$T_{S_i} = T_{l_i} \cap (T_{r_i} + T_{S_{i-1}}) \tag{7}$$

This last equation directly results from the space sum law for serial chains and the intersection law for parallel chains, see ([7]). Furthermore, since for any vector subspace **B**, **B**, $dim(\mathbf{A}) + dim(\mathbf{B}) = dim(\mathbf{A}+\mathbf{B}) + dim(\mathbf{A} \cap \mathbf{B})$, one gets:

$$\begin{aligned} m_i &= dim(T_{l_i}) + dim(T_{r_i} + T_{S_{i-1}}) - dim(T_{l_i} + T_{r_i} + T_{S_{i-1}}) \\ &= dim(T_{l_i}) + dim(T_{r_i}) + dim(T_{S_{i-1}}) - dim(T_{r_i} \cap T_{S_{i-1}}) \\ &\quad - dim(T_{l_i} + T_{r_i} + T_{S_{i-1}}) \\ &= l_i + r_i + m_{i-1} - 6 \end{aligned}$$

Since $m_0 = 0$, this recursive equation simplifies to:

$$m_i = \sum_{j=1}^{i} (l_j + r_j) - 6.i \tag{8}$$

The conditions (4),(5) and (6) can thus be written as

$$\forall i \in 1 \cdots n, \quad \sum_{j=1}^{i} (l_j + r_j) \geq 6.i \tag{9a}$$

$$\forall i \in 1 \cdots n, \quad \sum_{j=1}^{i-1} (l_j + r_j) + r_i \leq 6.i \tag{9b}$$

$$\sum_{j=1}^{n} (l_j + r_j) = 6.n \tag{9c}$$

Global isostaticity will be reach if we are able to find axis configurations preventing from the appearance of geometrical particularities (that will badly impact the kinematic equations system rank) for the L_j chain that verify the three conditions (9).

One can notice that (9c) points out the total number of l_j for the S_n mechanism, while (9a) gives the minimal value (to prevent from hyperstaticity in the sub-mechanisms S_j) for l_j and (9b) provides the maximal one (to prevent from internal mobility in the S_j).

Thanks to these last equations, we are able to calculate the different possible solutions for distributing the additional passive DOF at fixations over the structure:

- the possible choices for l_1 are such that $5 \geq l_1 \geq 6 - r_1$.
- for each choice of l_1, the possible choices for l_2 are such that $5 \geq l_2 \geq 12 - r_1 - r_2 - l_1$.
- for each choice of l_1 and l_2, the possible choices for l_3 etc.

This iterative reasoning leads to a tree that groups all the admissible combinations for l_i, as illustrated in Fig (4).

Out of this tree, many solutions are feasible from the point of view of mechanism theory but are not adequate for a correct transmission from an exosqueletton to a human member. This is why additional considerations are required to help the

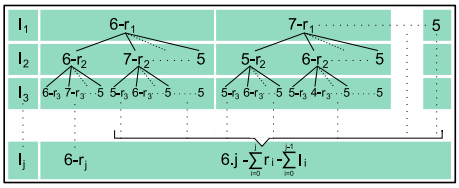

Fig. 4. Tree of possible solutions for the number of passive DoF to add at every fixation point

designer in selecting the appropriate DOFs for the fixations. These are illustrated in the next section on a particular example.

III. Application to a given exoskeleton

A. ABLE: an upper limb exoskeleton for rehabilitation

ABLE (see Figure 5) is a 4 axis exoskeleton that has been designed by CEA-LIST on the basis of an innovative actuation technology ([8]). Its kinematics is composed of a

Fig. 5. ABLE 4 axis exoskeleton actuated by screw-and-cable actuators

shoulder spherical arrangement made with 3 coincident axes and a 1 DOF pivot elbow. The forearm, terminated by a handle, is not actuated. Its kinematics is sketched in Figure 6. Most of the technological originality of ABLE comes from

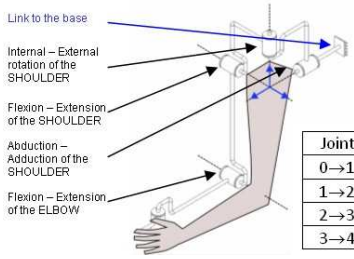

Joint	α_{i-1}	Θ_i	a_{i-1}	d_i
0→1	0	Θ_{1mes}	0	0
1→2	90°	$-\Theta_{2mes}$-90°	0	0
2→3	-90°	Θ_{3mes}-90°	0	0
3→4	0	Θ_{4mes}	357mm	0

Fig. 6. Kinematics of ABLE

its actuation and transmission system, which is based on a patented Screw-and-Cable system (SCS) [9]. The hardware characteristic of ABLE makes it an excellent platform for physical rehabilitation therapies. Its low joint stiffness and naturally compliant joints ensure the safety when using the robot for patients with physical disability. Unfortunately, first experiments shows us that without paying attention to the fixations by simply connecting arm and forearm middle areas to the orthosis using medical straps, which induce hyperstaticity, an alteration of natural movements appears [10]. This alteration is mainly due to a lack of synchronization between the arm joints: synergies seem to be perturbed even with an great transparency (low inertia and friction phenomenons).

B. Fixations design for ABLE

In this section, we apply general method proposed in Sec. II to ABLE. Firstly, since ABLE comprises an arm and a

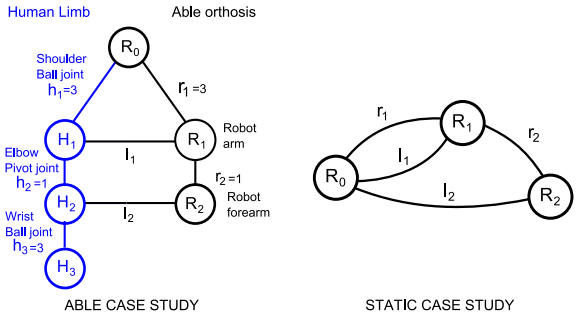

Fig. 7. Schematic of the ABLE and human arm coupling

forearm, we choose to use two fixations, one for each arm body (See Fig 7). The total number of passive DoF to be added is given by (equ. (9c)):

$$\sum_{j=1}^{n=2} l_j = 12 - \sum_{j=1}^{n=2} r_j = 12 - (3+1) \quad \Rightarrow l_1 + l_2 = 8 \qquad (10)$$

Morevoer, for the first fixation, the hyperstaticity avoidance constraint is (equ. (9a) and (9b)):

$$6 - r_1 \leq l_1 \leq 6 \quad \Rightarrow \quad 3 \leq l_1 \leq 5 \ .$$

In the case of only two fixations, since the total number of DOFs is fixed, the tree of possible solutions consists of parallel branches where l_1 is chosen between 3 and 5 and $l_2 = 8 - l_1$, which gives three couples for (l_1, l_2): (3,5), (4,4) and (5,3). It can be verified that these three couples verify of the constraints.

The derivation of the complete catalog of all possible arrangements among the three proposed distributions for the passive DOFs does not fit in the format of the paper. We here focus on three possible solutions that are represented in Figure 8.

The solutions (a) and (b) correspond to $(l_1 = 3)$ and $(l_2 = 5)$. This choice is somehow intuitive, because we have $l_i = 6 - ri$ for $i = 1, 2$, which mean that each subsystem S_i is independently chosen to be isostatic, resulting in a globally isostatic system. However, Solution (a) shall be rejected because the selected freed DOF (a ball joint at the fixation point P_1) lead to a lack of rank for the closed chain equations. Indeed, there is a possible internal motion that is a rotation around the axis joining P_1 to the center of rotation of the robot shoulder. Rather, Solution (b), which uses for the freed DOF at P_1 two rotations perpendicular to the arm axis and one translation along the arm axis should be used. Indeed, it

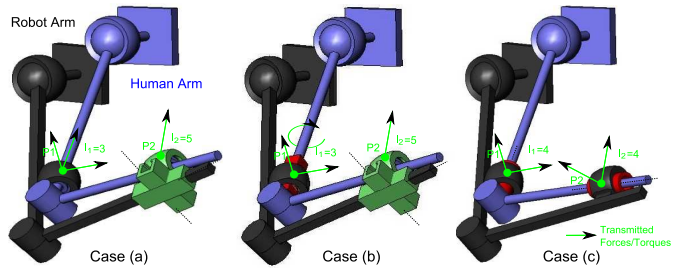

Fig. 8. Schematic of possibilities for coupling ABLE to an human arm. Case (a): ball joint alone at P_1 and ball joint on 2 slides at P_2; case (b): Universal joint + 1slide (in red) at P_1 and ball joint on 2 slides at P_2; case (c) Ball joints with slides (in red) at both P_1 and P_2.

can be verified that for Case (b) the closed loop kinematic equations for both S_1 and S_2 are of full rank.

However, for the practical realization, Solution (c) was kept. This solution involves $l_1 = l_2 = 4$ freed DOFs. It is less intuitive than the previous choice because S_1, taken alone, is a loop with $l_1 + r_1 = 7$ kinematic constraints, therefore the robot arm $\mathbf{B}_1$ connected through $\mathbf{L}_1$ to $\mathbf{H}_1$ has one degree of freedom even if $\mathbf{H}_1$ is unmoving. However, when the whole system is considered, there is no mobility for the exoskeleton if the human arm is kept still.

Solution (c) has the following advantage over solution (b): with solution (c), generating a moment to the human arm around the arm axis (D) is obtained by applying to opposite pure forces perpendicular to (D) at points P_1 and P_2; rather, with solution (b), it is directly transmitted to the upper arm through the fixation $\mathbf{L}_1$ (transmissible moment at P_1 around (D)). This is illustrated in Fig. 9. Applying directly this moment through a tight fixation is in fact a transmission by friction that can generate high tangential forces on the skin, and thus, pain. Note that the solution sketched in Fig. 9 is not

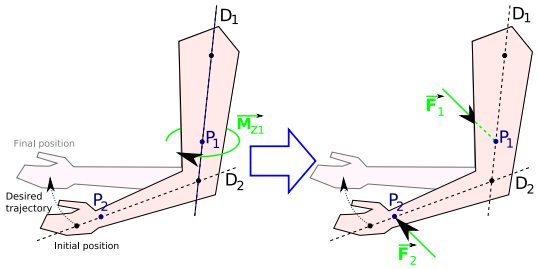

Fig. 9. Transmitting a moment around the upper arm axis with solution (b) (left) and (c) (right)

possible at full extension, where the two segment axes are aligned. In this case, the singular avoidance condition is not verified. This is not a problem in practice because ABLE is equipped with a range limit a few degrees befor full extension.

C. Fixations realization

To free three rotations and a translation at every fixation point, we un a ball joint mounted on a slide. We have transformed the standard ball-joint into a reduced (but fully functional) ball-joint mechanism allowing the subject arm not to be fully surrounded, which eases the installation and increases the freedom sensation. We have also placed the slide after the ball-joint mechanism in the kinematic chain, in such a way that the direction where no force can be transmitted is always the main direction of the human limb, no matter the amount of discrepancy appearing between ABLE links dimension and the subject arm dimensions. Two of these isostatic fixations were built in ABS with a rapid prototyping machine and the use of low profile linear guides (for the translation DoF). They were both fitted with one force sensor between the base and the 4 joints (ATI Nano43 6-axis Force/Torque sensor) allowing us to reconstruct the 3 forces and 3 torques components at P_1 and P_2 respectively).

For these experiments, the fixations were also equipped with a removable metallic pin trough all the fixation, allowing us to quickly lock the passive DoF without detaching the subject from the exoskeleton. This lock allows us to obtain a classical

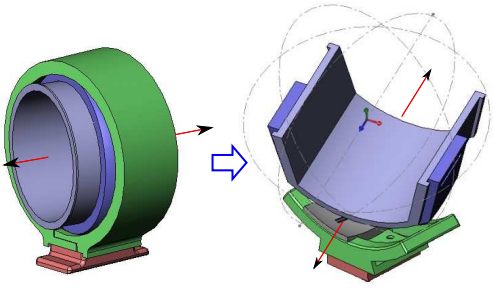

Fig. 10. Fixation simplification and realization

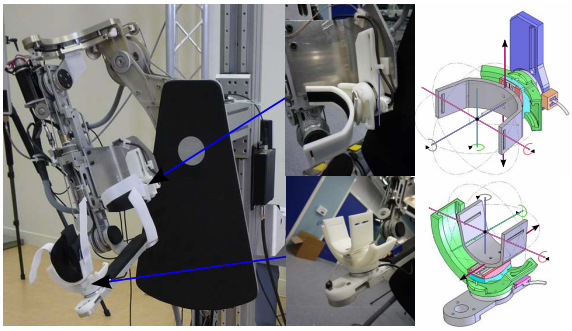

Fig. 11. The two fixations on the exoskeleton

fixation with no passive DoF and to compare the behavior of a subject attached to ABLE with or without fixations. These fixations were mounted on the 4 DoF Able exoskeleton at specific positions:

- The arm fixation is placed near the elbow, just under the triceps, in an area where the arm section do not vary too much during the elbow flexion/extension.
- The forearm fixation is placed near the wrist for the same reasons, and because the forearm section at this place is not round and allow to block the forearm to force the use of the fixation prono-supination DoF without strapping

firmly the tissues.

The possible motions left by the passive fixations have the following ranges:

DoF	Arm Fixation	Forearm Fixation
Rotation1	60°	120°
Rotation2	20°	20°
Rotation3	360°	360°
Translation	20mm	20mm

IV. Experimental evaluations

Two experimental campaigns were realized to quantify the hyperstatic forces level reached during a comanipulation of an arm inside a robotic exoskeleton. At the same time, the interaction improvement that such isostatic fixations can allow will be studied.

Healthy people were so asked to perform particular movements with their arm connected to the Able exoskeleton through the previously designed fixations. Exchanged force level at the interfaces were recorded, allowing us a transparency level quantification.

A. Control

We need to make the Able exoskeleton the more transparent we can, in order to quantify the force level due to hyperstaticity alone. Compensations were thus deployed on the robot, for the subject to perform natural unperturbed movements. The robot controller architecture is based on a PC104 board with two endowed 3 channel axis controller. It runs at 1kHz the control law thanks to a real time operating system (RTlinux). As the Able exoskeleton is only fitted with optical encoders, we have do not have access to an acceleration signal. The transparency is thus achieved by an experimentally identified gravity compensation for all axis and also by compensating for the residual dynamic dry friction compensation. This residual friction compensation has been developed in order to blend the friction phenomenons on all axis, and so on not to lead subject to do non-natural moves because of feelings differences on every joints.

Another controller based on a PC104 board with two Analog and Digital I/O PCI card (Sensory 526) is used for acquiring the readings of the F/T sensors during the exercise every 5ms (RTAI real time operating system).

B. Experimental setup

During all the experiments, we assume the exoskeleton to be ”transparent” due to the gravity and friction compensation. Analyzing the interaction force and torque variations at the interfaces during the same movement with isostatic fixations and without (locked case) will allow us to evaluate their impact on preventing for the appearance of uncontrolled forces and thus, on the general transparency level but also to quantify them roughly.

The subject is asked to follow a metallic wire with a complex shape with a metallic stem from one end to another and inversely. The system is ”electrified” so that the subject is told by a sound when the contact between the wire and the stem is lost. This exercise allows to study the impact of the passive DoF fixations on general moves because it needs the subject to use all his arm joints to be completed.

Before recording the trajectory and force data, the subject was asked to perform the exercise several times in order to learn how to use the exoskeleton and not to observe learning phenomenon during the recorded three movement repetition.

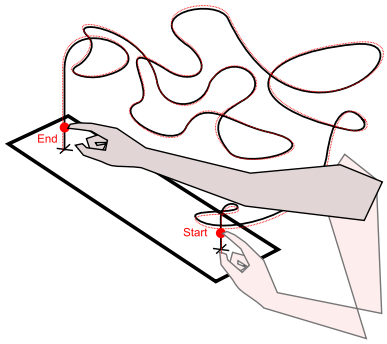

Fig. 12. Complex 3D following task

V. Results and discussions

This campaign was held on 18 healthy naive subjects. Principal results are presented below. In Figure 13, we plotted

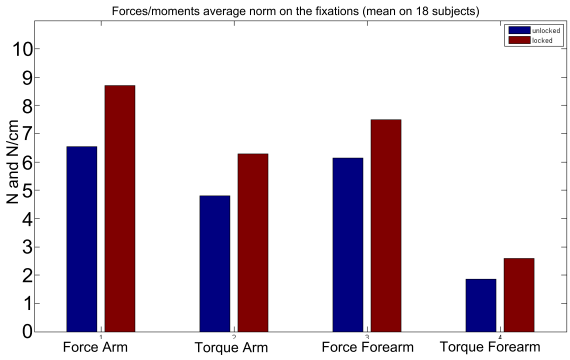

Fig. 13. Forces/torques average norme on the fixations (mean on 18 subjects) Blue unlocked and red locked

the represents the force and torque norm mean during the experiments, for the two sensors, averaged across the eighteen subjects(the torque is computed at the rotation center of the fixation). We can observe a decrease in the interaction force level by 25% for the arm fixation and by 20% for the forearm. If we observe the mean of each force and moment absolute value for the sensors (Figure 14), we can more precisely analyze the phenomena. One particular phenomenon is the arm torques measured around the Z axis that seem to stay at a very low level during the experiments. These reduced decreases of some components can be linked with a phenomenon observed during these experiments: a push-pull phenomenon between the part because of the usury of the plastic parts. We cannot quantify the phenomenon impact, but it has surely lead to decrease the performance of these

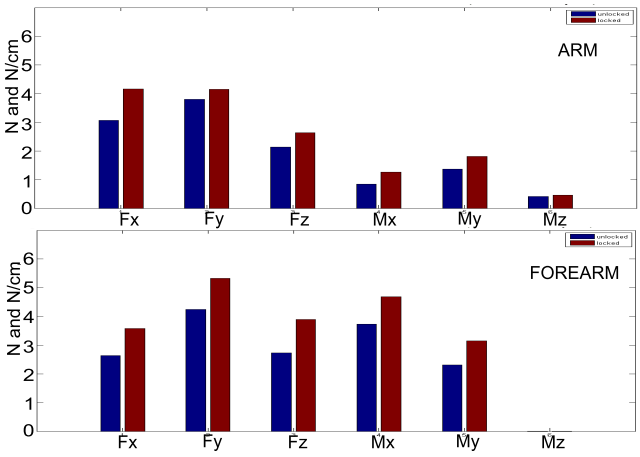

Fig. 14. Mean of each force and moment absolute value for the two sensors. Blue unlocked and red locked

fixations.
Although these preliminary mixed results appears promising, we realize that the task was too endpoint oriented to force the subject to perform the same trajectory (same speed and path). Only the start and end areas are really constrained, so the subject can completely transform or adapt -even unconsciously- his arm trajectory. This path alteration thus limits our comparison between the two fixations modes.

A. Discussions

Our preliminary and simple fixations, even mechanically limited, helped to reduce the hyperstatic uncontrolled and undesired interaction force level up to 25 per cent compared to classic rigid fixations. What is important is that our approach seems to be consistent. Beside the liberation of DoF along the human limb advocated by several researcher teams, it is really the hyperstaticity phenomena we studied that is targeted: Indeed, we achieve to even more reduce the interaction force level by also liberating the rotation DoF, what proves that reaching isostaticity in the coupling can improve interaction.

This method allows to design fixations that preserve human mobility. These fixations, if they were perfectly isostatic and with any friction (and that gravity and firction compensation were ideally perfect), will lead to the disappearance of some forces and torques (Fx, Mx, My and Mz in our case), only allowing the transmission of the desired forces on the ABLE exoskeleton case. Alas, in our experiment, even if the level of the 4 other interaction forces/torques is reduced (see Fig. 13), it stay still important even with the passive added DoF. More than the fact that it is very difficult to ask subject to perform the same joint trajectory with a varying robotic configuration, several other explanations can be formulated to explain the system performance limitations:

- the plastic realization of the fixation,
- the limited workspace of the passive DoF (notably for the translation),
- the appearance of uncontrolled and undesired contact point during the movement, leading to a partial read of the exchanged force level on the sensors

Theses hypothesis will be verified in future experimental campaigns.

Beside these quantitative results, all the subjects mentioned they feel more comfortable with the passive DoF released. An interesting campaign should be perform in the future to fit the subject with motion capture sensors and record the task movement with the robot (and the two fixations states) and without. Comparing the trajectory realized by the free arm to the ones followed when connected to the robot could help to quantitatively describe the benefit of isostatic fixations in the ”task space” rather than in the ”force space”: balancing the forces data with a coefficeint describing the path variation with and without the fixations liberated could help to obtain realist results.

VI. Conclusion

In this paper we presented a methodology aimed at designing the kinematics of fixations between an exoskeleton and a human member. The provided solution avoids hyperstaticity but also adapts to large variations on the human limb geometry without requiring a complex adaptable robot structure. Thanks to this method, we prototyped isostatic fixations prototypes for a 4 DoF exoskeleton and experimentally verified their benefit on minimizing uncontrollable hyperstatic forces at the human robot interface.
These first results show that hyperstatic constraints lead to not negligible uncontrolled force appearance at the interface. To our knowledge, this is a first experiment showing that benefit. Interestingly, the addition of passive degrees of freedom can be done through light, compact an unexpensive mechanisms. In the case of ABLE, it is estimated that the passive mechanism cost is about one 30th of the overall robot cost. In that sense, the reduction of 20 to 25% of the force magnitude resulting from the installation of the device brings a worthy benefit.
Current work consists of fabricating better quality fixations, exhibiting less friction, to run a new campaign under better experimental conditions.

Acknowledgments

This work was supported in part by the A.N.R. (Agence Nationale de la Recheche) with the projet BRAHMA (BioRobotics for Assisting Human Manipulation) PSIROB 2006.

Appendix

Demonstration of Proposition 1

1) Conditions (3) are sufficient : $[(3) \Rightarrow (2)]$.
Equation (3c) naturally requires condition (2a) on the velocities to be respected for $i = n$: ${}^{S_n}T_{S_n} = \{0\}$. Furthermore, if we suppose that ${}^{S_n}T_i = \{0\}$, then body $\mathscr{R}_{i-1}$

is linked to a fixed body through two sub-mechanisms S_{i-1} and R_i. So

$$^{S_n}T_{i-1} =^{S_{i-1}} T_{i-1} \cap T_{r_i} = T_{S_{i-1}} \cap T_{r_i} = \{0\}$$

thanks to hypothesis (3b). We thus have a recurrent relation:

$$^{S_n}T_i = \{0\} \Rightarrow^{S_n} T_{i-1} = \{0\} \ .$$

This relation is true for $i = n$ (because of (3c)). Therefore, it is true $\forall i \in 1 \cdots n$. Condition (2a) is thus verified $\forall i \in 1 \cdots n$, thanks to hypothesis (3b) and (3c).
Consider now Eq. (3a). For $i = n$, it writes:

$$dim(T_{S_{n-1}} + T_{r_n} + T_{l_n}) = 6.$$

Considering the loop $\mathscr{R}_0 \rightarrow \mathscr{R}_{n-1} \rightarrow \mathscr{R}_n \rightarrow \mathscr{R}_0$ in Fig. 3 and the kinemato-static duality principle, we have:

$$dim(^{S_n}W_{ln\rightarrow 0}) + dim(T_{S_{n-1}} + T_{r_n} + T_{l_n}) = 6.$$

So $dim(^{S_n}W_{ln\rightarrow 0}) = 0$, requiring that condition (2b) is verified for $i = n$. Assume now that (2b) is verified for $\forall j \in i+1 \cdots n$. Writing equilibriums for bodies $\mathscr{R}_n$, $\mathscr{R}_{n-1}$, ...,$\mathscr{R}_{i+1}$ successively shows that all the forces are null in the entire mechanism $\bar{\mathscr{S}}_i$, which is defined as the complementary to $\mathscr{S}_i$ in $\mathscr{S}_n$. This leads to:

$$^{S_n}W_{ln\rightarrow 0} =^{S_i} W_{li\rightarrow 0}.$$

In this case, condition (3b) which implies that $^{S_n}W_{ln\rightarrow 0} = \{0\}$ also implies that (2b) is verified for i. In summary, we know that, according to (3a):

- (2b) is verified for $i = n$,
- if it is also verified for $\forall j \in i+1 \cdots n$, it is also verified $\forall i$

It is thus verified $\forall i \in 1 \cdots n$.

2) Conditions (3) are necessary : $\left[\overline{(3)} \Rightarrow \overline{(2)}\right]$.
Firstly, if condition (3c) is not verified, then obvisouly (2a) and (2b) neither, because then

$$^{S_n}T_n = T_{S_n} \neq \{0\}.$$

If (3b) is not verified, then

$$\exists i, \ (T_{r_i} \cap T_{S_{i-1}}) \neq \{0\},$$

and even if i is fixed, it exists a possible move for $(i-1)$, i.e. $^{S_n}T_{i-1} \neq \{0\}$. Conditions (2a) and (2b) are thus not verified.
If (3a) is not verified, i.e. that

$$\exists i, \ dim(T_{S_{i-1}} + T_{r_i} + T_{l_i}) \leq 6,$$

then $^{S_i}W_{li} \neq \{0\}$. We have two solutions:

- $^{S_n}W_{li\rightarrow 0} =^{S_i} W_{li\rightarrow 0}$ and so on $^{S_n}W_{li\rightarrow 0} \neq \{0\}$ and condition (2a) is not repected,
- $\exists j > i$, $(^{S_n}W_{lj\rightarrow 0} \neq \{0\}$ and then once again condition (2a) is not respected.

In conclusion (3a), (3b) and (3c) are necessary.

REFERENCES

[1] Jose L. Pons. *Wearable Robots: Biomechatronic Exoskeletons*. 2008.
[2] Scott SH and Winter DA. Biomechanical model of the human foot: kinematics and kinetics during the stance phase of walking. *J Biomech.*, 21993.
[3] Van der helm, Veeger, and Pronk HG. M. Geometry parameters for musculoskeletal modelling of the shoulder system. *Journal of biomechanics*, June 1992.
[4] A. Schiele and F.C.T. van der Helm. Kinematic design to improve ergonomics in human machine interaction. *Neural Systems and Rehabilitation Engineering, IEEE Transactions on*, 14(4):456–469, Dec. 2006.
[5] C. Diez-Martnez, J. Rico, J. Cervantes-Snchez, and J. Gallardo. *Mobility and connectivity in multiloop linkages*, pages 455–464. 2006.
[6] Stokdijk M.[1], Meskers C.G.M., Veeger H.E.J., de Boer Y.A., and Rozing P.M. Determination of the optimal elbow axis for evaluation of placement of prostheses. *Clinical Biomechanics*, March 1999.
[7] K.J. Waldron. The constraint analysis of mechanisms. *Journal of Mechanisms*, pages 101–114, 1966.
[8] P. Garrec, J.P. Friconneau, Y. Measson, and Y. Perrot. Able, an innovative transparent exoskeleton for the upper-limb. pages 1483–1488, Sept. 2008.
[9] P. Garrec, JP. Martins, and JP. Friconneau. A new technology for portable exoskeletons. *AMSE2004*, 2004.
[10] N. Jarrasse, J. Paik, V. Pasqui, and G. Morel. How can human motion prediction increase transparency? May 2008.